IEEE Access
Multidisciplinary ⋮ Rapid Review ⋮ Open Access Journal

Received 19 June 2024, accepted 28 July 2024, date of publication 1 August 2024, date of current version 30 August 2024.

Digital Object Identifier 10.1109/ACCESS.2024.3436829

RESEARCH ARTICLE

RT-NeuroDDSM: Real-Time EEG-Driven Diagnostic Decision Support Model for Neurological Disorders Using Deep Learning

RUCHI MITTAL[1], R. JOHN MARTIN[2], HAMDAN ALSHEHRI[2], VARUN MALIK[1], (Member, IEEE), S. B. GOYAL[3], (Senior Member, IEEE), S. L. SWAPNA[4], HAITHAM ASSIRI[2], AND SALAHALDEEN DURAIBI[2], (Member, IEEE)

[1]Chitkara Institute of Engineering and Technology, Chitkara University, Chandigarh, Punjab 140401, India
[2]College of Engineering and Computer Science, Jazan University, Jazan 45142, Saudi Arabia
[3]Faculty of Information Technology, City University Malaysia, Petaling Jaya 46100, Malaysia
[4]Applexus Technologies, Thiruvananthapuram 695581, India

Corresponding author: Hamdan Alshehri (halshehri@jazanu.edu.sa)

ABSTRACT The internet of medical things (IoMT) has become a pivotal aspect of IoT applications, playing a crucial role in cutting down healthcare expenses, enhancing access to clinical services, and refining operational efficiency within the healthcare domain. An early detection of neurological brain disorders continues to present a formidable challenge. In response, our research endeavors are directed towards the IoMT-based system used for the real-time diagnosis of neurological disorders. In this paper, IoMT-based real-time diagnosis model is developed for neurological brain disorders using systematic deep learning and electroencephalogram (EEG) signal (RT-NeuroDDSM). We first introduce the time domain, channel and spatial attention network (TCSNet) for feature extraction which extracts the high-level time series, channel and spatial features, respectively. TCSNet aims to learn more valuable features from the input data to achieve good classification results. Furthermore, in order to maximize features, we create the modified normative fish swarm (MNFS) feature selection algorithm. Next, the detection of various neurological brain problems, including neuro-typical, epilepsy, and autism spectrum disorder (ASD), is accomplished by applying the hinging hyperplane neural network (HHNN). To verify the performance, we used the publicly accessible EEG datasets from University of Bonn-Germany, CHB-MIT EEG repository, and King Abdulaziz University. The RT-NeuroDDSM has an overall classification accuracy of 99.956%, making it 5.471% more in efficiency compared to the existing state-of-the-art model.

INDEX TERMS Autism, biomedical signal processing, deep learning, digital healthcare, electroencephalography, epilepsy, Internet of Medical Things.

I. INTRODUCTION

The Internet of Medical Things (IoMT)-based smart healthcare system is made up of several online-connected and networked smart medical devices [1], [2]. A smart healthcare system based on IoMT has multiple phases. Medical data from the patient's body will be gathered using smart sensors integrated into implanted or wearable smart devices connected via a wireless sensor network (WSN) or body sensor network (BSN) [3]. Following its acquisition, the medical data can be examined using an appropriate AI-based method for data transformation and interpretation [4]. In the event

The associate editor coordinating the review of this manuscript and approving it for publication was Siddhartha Bhattacharyya.

of major problems, intelligent AI-based smartphone applications can assist in contacting physicians or other medical needs. Brain problems are referred to as neurological brain disorders, which are a subgroup of human illnesses [5]. Knowledge has led to a drop in the death rate from a number of long-term brain diseases, yet these conditions can still result in partial or permanent disability. Electroencephalography (EEG) signals provide a representation of the electrical activity within the brain [6]. Employing signal processing techniques for EEG signal analysis is fundamental in clinical practice for the surveillance and diagnosis of neurological disorders such as autism spectrum disorder (ASD) and epilepsy [7]. This significance stems from EEG data's ability to unveil abnormalities in neuronal electrical activity. Given the intricate nature of the human brain, it harbors a wealth of information pertinent to limbic functions and neurological pathology [9]. Neurologists and other skilled medical professionals presently use EEG data to manually detect most brain ailments [8], [9], [10]. Over 600 diseases affect the neurological system, including brain tumors, neuro infections, epilepsy, dementias, Alzheimer's, stroke, multiple sclerosis, Parkinson's, migraines, and traumatic disorders like autism and brain trauma [11]. A significant amount of research is currently being done in this area [12], [13], [14], [15], [16], [17], [18], [19], [20] in an effort to develop and enhance a diagnostic for neurological brain diseases. A persistent brain condition that affects individuals of all ages is epilepsy. Recently, several deep learning (DL) techniques for epilepsy diagnosis have been published [12], [13], [14], [15], [16]. The EEG signal is cleaned up from noise and artifacts using a band-pass filter and manual noise rejection [12]. Channels were then chosen using a variety of transform analysis techniques, including spectrogram, Wigner-Ville distribution, and continuous wavelet transform, based on statistical features and correlation. To improve the classification accuracy and prediction rate, an adaptive grey wolf optimizer (AGWO) acquires and enhances the attributes [13]. The aim is to improve the epilepsy prediction rate by adaptively merging the auto-encoder concept with genetic algorithms (GA) to optimize characteristics. The transformer model called EpilepsyNet, which is based on deep learning, was trained using 35 channels of EEG data [14]. CNN and the tunable-Q wavelet transform are utilized in a real-time EEG model to detect epileptic episodes. The temporal domain and frequency domain characteristics of the EEG were highlighted using statistical moments and spectral band power [15]. A wearable, lightweight seizure detection device called LightSeizureNet (LSN) [16] uses raw EEG data to detect epileptic seizures in real time.

The brain connectivity matrix was constructed using an approximation derived from neural networks [17]. A cross-sectional analysis was performed on 69 children who were enrolled in the ASD early diagnostic program and had both a clinical diagnosis and an electroencephalogram [18]. Infants aged 6 and 12 months who are more likely to develop ASD and LLI should have baseline EEG spectral power defined compared to typically developing infants [19]. The method of detecting ASD is called Chronological Stitching Training Optimization-Deep Residual Network (CSTO-DRN); DRN is pre-trained using the CSTO methodology by adjusting the ideal weights [20]. The diagnosis of individual neurological brain illnesses has been the subject of numerous investigations. To our knowledge, nevertheless, not much research has been done on the problem of concurrently identifying several neurological brain illnesses. In this study, we have integrated a systematic deep learning framework with EEG signals to construct the IoMT-based real-time diagnosis model for neurological brain illnesses, which we call RT-NeuroDDSM. The originality of our work can be summed up as follows:

1. For feature extraction, we employed the time domain, channel, and spatial attention network (TCSNet) to extract high-level time series, channel, and spatial features. By using TCSNet, our aim is to extracts valuable insights from the input data, thereby facilitating robust classification outcomes.
2. To address data dimensionality challenges, the modified normative fish swarm (MNFS) algorithm for feature selection. It optimizes the selection of features, mitigating issues associated with high-dimensional data representation.
3. Furthermore, we employed the hinging hyperplane neural network (HHNN) for the detection of multiple neurological brain disorders, including neuro-typical, epilepsy, and ASD. It effectively discern between various neurological conditions, thereby enhancing diagnostic accuracy.
4. To verify our model's effectiveness, we used publicly accessible EEG datasets from King Abdulaziz University, CHB-MIT, and Bonn University Hospital. Our goal is to show the effectiveness and dependability of our RT-NeuroDDSM in practical diagnosis settings by means of extensive testing on these datasets.

The rest of this paper is organized as follows: Section II delves into the review of the neurological brain disorders diagnosis system and explores the research gaps. Section III addresses the challenges encountered in the neurological brain disorders diagnosis using the proposed RT-NeuroDDSM method. Section IV presents the outcomes and a comparative analysis, demonstrating the effectiveness of the proposed RT-NeuroDDSM method. Finally, in Section V, we draw conclusions.

II. RELATES WORKS

Several previous studies have investigated EEG-based diagnosis techniques for neurological brain disorders, including Healthy, epilepsy, and ASD. Table 1 summarizes the research gaps gathered from the previous research works.

A. REVIEW ON EPILEPSY DIAGNOSIS

A practical approach for early epilepsy identification is proposed in [21], utilizing feature extraction and categorization techniques. By employing the DWT method to dissect the

signal components, the characteristics are obtained. To narrow down the dimensions and concentrate on the highly significant features, PCA and the t-SNE algorithm were applied. These phases produced features that were used as input for the extreme gradient boosting, K-NN, DT, RF, and MLP classifiers. With DWT and PCA, the RF classifier yielded 97.96% accuracy, 99.1% precision, 94.41% recall, and 97.41% F1 score. A seizure-detection system for activities of daily living (ADL), utilizing specific EEG channels, has been developed. The system presented in [22] encompasses several elements, including the identification of the predominant channel for interpreting XLtek EEG data. The ensuing combined datasets are then subjected to testing and evaluation using a deep learning model employing 1D-CNN, Bi-LSTM, and attention mechanisms. The outcomes revealed an accuracy of up to 96.87%, precision of 96.98%, and sensitivity of 96.85%. Additionally, a long short-term memory (LSTM) network [23], typically used with the Bonn Epilepsy dataset, was employed to enhance performance. According to preliminary evaluation, the LSTM performs well, with impressive rates of over 95% accuracy in classification tests, 100% accuracy in binary classifications, and above 93.5% overall. A smartphone application to track the categorization of EEG data was created in conjunction with the development of an improved and effective epileptic seizure method utilizing EEG signals [24]. All connected users receive a notification and visual alert if an EEG signal is determined to be epileptic. It outperformed recently published studies with an average classification accuracy of 98% using machine learning (ML) approaches. Brain activity utilizing EEG data is evaluated using a residual network model (ResNet-BiGRU-ECA) to accurately discern epileptic seizures [25]. The trial findings show that the ResNet-BiGRU-ECA model outperformed the most sophisticated DL models, with an accuracy rate and F1-score of 0.998. The enhanced grey wolf approach and variational modal decomposition (VMD) were used to identify epileptic EEG patterns [26]. A support vector machine (SVM) classifier was used to correctly detect epileptic EEG patterns in the data. The results show that 98.3% accuracy, 98.9% sensitivity, and 98.5% specificity are obtained with the VMD-SVM technique.

B. REVIEW ON ASD DIAGNOSIS

A DL-based autism diagnostic process is used in conjunction with a pre-trained auto-encoder model for feature extraction, along with a ensemble optimization approach for scattered and unpolished data [27]. An auto-encoder-based hybrid optimization technique is used for feature extraction from the acoustic feature data set Geneva Minimalistic Acoustic Parameter Set (eGeMAPS). EEG, which measures electrical activity in the brain, is a useful diagnostic tool for autism [28]. The pre-processed signals underwent transformation into two-dimensional representations using the higher-order spectra (HOS) bispectrum. Subsequently, nonlinear properties were mitigated through the application of locality sensitivity discriminant analysis (LSDA). Employing the probabilistic neural network (PNN) classifier resulted in the attainment of the highest accuracy, reaching 98.70% while utilizing only five features. Specifically, electrodes F3, F4, P7, and P8 were utilized for characteristic extraction from the EEG data and computation of the band power spectrum density [29]. Next, use these features to evaluate multiple machine learning models.

The multi-layer perceptron neural network model (MLP-NN) exhibits elevated performance metrics, boasting an Area under the Curve (AUC) value of 0.9299, a Cohen's Kappa coefficient of 0.8597, a Matthews coefficient of 0.8602, and a Hamming loss of 0.0701. This indicates its robustness in classifying data instances within the given classification problem. Five pre-trained CNNs are used as feature extractors and a DNN model as a binary classifier to accurately diagnose autism in children [30]. An 88% NPV, 88.46% sensitivity, and 96.63% AUC are produced by the Xception model. The probabilistic neural network (PNN) classifier demonstrates remarkable accuracy, achieving a rate of 98.70% while utilizing only a limited set of five features. It is crucial to employ electrodes F3, F4, P7, and P8 for the computation of band power spectrum density [29], as this process enables the extraction of pertinent characteristics from EEG data. Subsequently, these extracted features are employed to assess various machine learning models. Among these models, the multi-layer perceptron neural network (MLP-NN) stands out with exceptional performance metrics, including an AUC value of 0.9299, Cohen's Kappa coefficient of 0.8597, Matthews coefficient of 0.8602, and a Hamming loss of 0.0701. This signifies the MLP-NN's efficacy in accurately categorizing data instances, underscoring its suitability for robust classification tasks within this domain. Five convolutional neural networks (CNNs) pre-trained for feature extraction purposes are employed, alongside a deep neural network (DNN) model utilized as a binary classifier for accurate autism identification in children [30]. Notably, the Xception model yields robust performance metrics, including an 88% Negative Predictive Value (NPV), 88.46% sensitivity, and an impressive AUC of 96.63%. Conversely, the EfficientNetB0 model consistently produces a prediction score of 59% for both autistic and non-autistic groups at a 95% confidence level. In a sensor-based system for early autism detection, feature extraction for precise classification is made possible by an energy-efficient signal modification technique [31]. The results showed that 96% of the used ML models had 100% sensitivity, 95% accuracy, and 95% F1 score. The variational mode decomposition (VMD) method for P300 signal detection uses ASD subjects [32]. The synthetic minority oversampling method is used to enrich data in order to address the problem of class imbalance. The VMD mode with SVM classifier performed the best, with an accuracy of 91.12%.

C. SUMMARY OF RESEARCH GAPS

As the primary cause of death globally, brain illnesses present a significant challenge to global health. Although the analysis

TABLE 1. Bench marking existing studies on epilepsy and autism diagnosis.

Methodology	Ref.	Feature extraction	Classification	Dataset	Accuracy (%)	Research gaps
Epilepsy diagnosis	[21]	DWT, PCA	K-NN,RF, DT	UCI	97.96	Time consuming process
	[22]	XLtek EEG	1D-CNN, Bi-LSTM	King Abdulaziz University	96.87	Unbalanced as a result of fewer EEG readings
	[23]	CWT	LSTM	Bonn University	93.5	Data visual analysis has grown more difficult.
	[24]	FIR filter	K-NN and SVM	Bonn University	98	Theoretical techniques has resulted in poor practical
	[25]	UNet	ResNet-BiGRU-ECA	ESRD	99.8	Leads to overfitting challenges when insufficient data
	[26]	VMD and VMF	SVM	CHB-MIT	98.3	Overfitting problem
Autism diagnosis	[27]	eGeMAPS	SVM, BLSTM	SNUBH	68.18	Huge complexity
	[28]	HOS and LSDA	Probabilistic neural network (PNN)	CARS, ATEC, PEP3, SRS	98.70	Accessibility and interpretive bias
	[29]	TBR, TAR, PSD	MLP-NN	Emotiv website	92.99	Face data dimensionality issue
	[30]	MobileNet,EfficientNetB2	DNN	Autistic children	95	This process is long-winded because of complex process
	[31]	Welch and DWT	SVM, LR and decision tree	SNUBH	96	Not consider the process of optimal feature selection
	[32]	Variational mode decomposition	EBT, SVM, ANN	BCIAUT-P300	91.12	An unbalanced dataset causes the overfitting problems

of electroencephalograms (EEGs) is essential for the diagnosis of brain illnesses, medical professionals may find it difficult to decipher complicated EEG patterns and arrive at a diagnosis. However, the shortcomings of the state-of-the-art techniques currently in use limit their overall efficacy. Furthermore, they focus on examining a single dataset, which may cause them to ignore the complexity and inherent diversity of EEG patterns linked to depression. Additionally, some approaches use DL techniques that have exponential time complexity, which makes the training both computationally and time expensive. Consequently, their practicality and applicability in real-world scenarios are compromised. From the literature review [21], [22], [23], [24], [25], [26], [27], [28], [29], [30], [31], [32], we learned that a large number of studies have focused on the individual diagnosis of neurological brain disorders. To the best of our knowledge, there is, however, a dearth of research that focuses on the difficulty of simultaneously diagnosing several neurological brain problems. To summarize, the following research gaps are highlighted by our review.

- Most of the techniques face the computational complexity also they need massive amount of data for training which causes the under fitting problem
- Still overfitting problems are not solved yet because of unbalanced training data, thus those techniques suitable only for known training data
- Most of the works not address the optimal feature selection due to incorrect labeling data which causes the data dimensionality issues
- The decision-making processes of ML/DL techniques face interpretability issues limited by the design of hidden layers.

To address these problems, we present the IoMT-based real-time diagnosis model for neurological brain disorders using EEG signals (RT-NeuroDDSM). The main objective of proposed model is used to detect and classify multiple neurological brain disorders in the single system. Moreover, we address the feature optimization by using the optimal feature selection which reduces the data dimensionality issues.

III. METHODS

Figure 1 outlines the comprehensive approach to diagnosing neurological brain disorders using DL techniques with EEG signals. Initially, the IoMT facilitates the gathering of raw EEG signals directly from patients with neurological conditions. These signals are then stored in a cloud server, enabling centralized and efficient data management. Leveraging established datasets from institutions like Bonn University, CHB-MIT, and King Abdulaziz University provides a diverse range of EEG recordings for analysis and model training. Subsequently, the raw EEG signals undergo preprocessing to enhance their quality and remove any noise

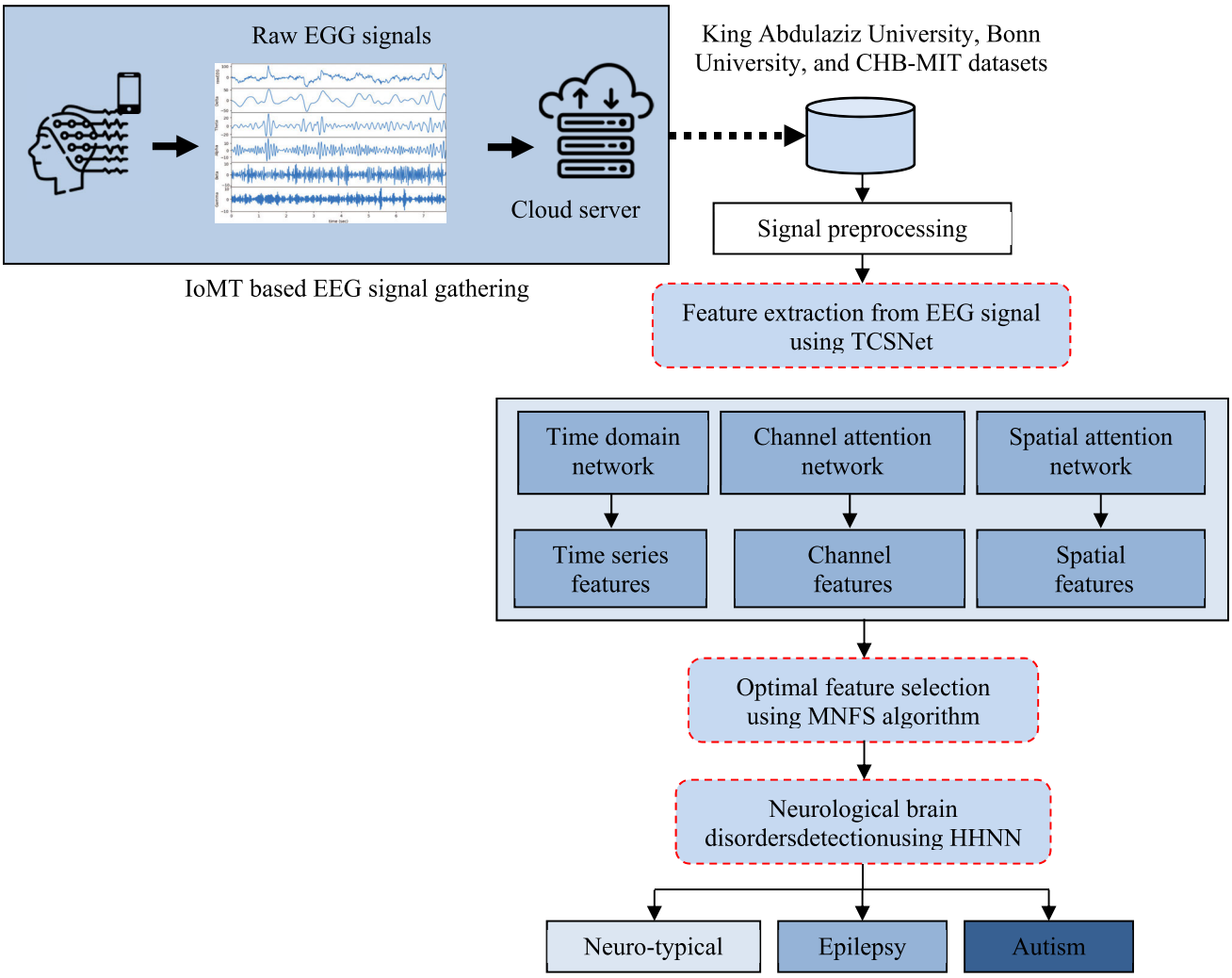

FIGURE 1. Neurological brain disorder diagnosis (RT-NeuroDDSM) model proposed in this study.

or artifacts. Feature extraction plays a crucial role in capturing relevant information from the EEG signals. This is achieved through a combination of techniques, including the time domain channel spatial network (TCSNet) for extracting time-domain features, a channel attention network for capturing channel-specific features, and a Spatial Network for extracting spatial features. The extracted features are then subjected to optimal feature selection using the modified normative fish swarm (MNFS) algorithm, which identifies the most informative features for model training. Finally, a hinging hyperplane neural network (HHNN) utilizes the selected features to classify EEG signals and diagnose neurological disorders accurately. By integrating these steps, the proposed approach offers a comprehensive and effective method for diagnosing neurological brain disorders using DL and EEG signals.

Real-World Application of RT-NeuroDDSM: In clinical settings, this model can greatly enhance the early and accurate diagnosis of neurological disorders. Early detection is crucial for timely intervention and can lead to improved patient outcomes, particularly in the management of conditions such as epilepsy and autism spectrum disorder (ASD). By providing a reliable diagnostic tool, clinicians can make more informed decisions, potentially reducing the severity of symptoms through earlier treatment. Additionally, the RT-NeuroDDSM model can be integrated into portable EEG monitoring devices, enabling continuous, real-time monitoring for individuals at risk of neurological disorders. This capability is especially beneficial in remote and underserved areas, where access to specialized neurological care is limited. Real-time monitoring allows for the immediate detection of abnormalities, which can prompt swift medical responses and reduce the risk of adverse events. Moreover, the model's high accuracy and efficiency make it a valuable tool for research and development in the field of neurology. Researchers can use RT-NeuroDDSM to gain deeper insights into the progression of neurological disorders and the impact of various treatments. This can lead to the development of more effective

therapeutic strategies and improve the overall understanding of these complex conditions. The RT-NeuroDDSM model also holds potential for integration with other IoMT devices, creating a comprehensive network of medical monitoring tools. This interconnected system can provide a holistic view of a patient's health, combining data from multiple sources to offer more accurate and detailed diagnoses. Such a system would be instrumental in advancing personalized medicine, tailoring treatments to the specific needs of each patient based on continuous health data monitoring.

A. FEATURE EXTRACTION USING TCSNet

The time domain channel spatial network (TCSNet) serves as a pivotal component in the feature extraction. It is specifically designed to capture high-level features from EEG signals across three key dimensions: time, channel, and spatial features. In the time domain, TCSNet focuses on extracting temporal patterns and dynamics inherent in EEG signals. These techniques enable TCSNet to identify minute variations and patterns in the EEG signals that might be suggestive of neurological conditions. The filter data sequence in a channel attention network is calculated as follows: N represents bunch size, inch indicates the number of channels, and time and test, respectively, address information examining point and time duration. We utilize one scale CNN to get one layered include portrayal $E^{M*in-cg*1*1}$. Moreover, The $1*1$ convolution is be used for actuation capability.

$$D_S = Leaky\,Relu\,(D_v) \in E^{M*in-cg*1*1}. \tag{1}$$

The channel consideration worth can be determined as follows.

$$D_{VS} = ADD\,(D, D_S) \in E^{M*in-ch*time*sampe}. \tag{2}$$

The new feature matrix is created by combining the dense layer's output and the matrix's input in this paper's alternative data connection method. Zk has received the component guides of all layers preceding it, as a consequence of the model outcome.

$$Zk = gk\,([Z_0, Z_2, Z_3])\,, \tag{3}$$

The underlying learning rate is 0.001, and the unfortunate thing about the model preparation process is the iterative cross-entropy misfortune capability to prepare the organization.

$$loss = -\sum_{0=1}^{V}\sum_{V=1}^{V} u_{o,d}\log\left(o_{p,v}\right). \tag{4}$$

Among them, addresses the quantity of classes, addresses the group preparing size and y addresses the right hot coding. At the point when the class mark c is steady with the anticipated class mark, In order to reduce model over fitting, dropout is set to 0.5.

We use the channel-wise EEG signals v_u in the spatial attention network by passing them through a convolutional layer and then a maximum pooling layer. This stage is similar to a front-end for a recurrence study that extracts data from the time-space signals that v_u shows in the manner described below.

$$e_u = Max\ (elu\ (Conv\ (v_u))) \tag{5}$$

where the convolution operation is denoted by $Conv\,(v_u)$, and the activation function is an exponential linear unit called elu. Max. The gating component dynamically determines which EEG channels to assign divided loads to. To specify the gating component and achieve a non-straight planning, the following two completely connected layers are used:

$$N_A = elu\ \ (q_2\ \ (elu\ \ (q_A w_a + v_1)) + v_2) \tag{6}$$

where $w_a + v_1$ represents each of the first and second fc layers' unique boundaries. The propensity terms of two fully linked layers are denoted by b1, b2. The consideration cover that the spatial consideration instrument creates is called Ms.

$$D' = N_A \oplus R \tag{7}$$

where M signifies a point-wise increase. During the duplication, the consideration esteem is communicated along the worldly aspect, i.e., $D' = N_A \oplus R$ Finally, we employ a maximum pooling layer after a convolution layer to eliminate the spatial component depiction from the covered EEG signals.

B. FEATURE OPTIMIZATION USING MNFS ALGORITHM

Feature optimization is the process of eliminating extraneous or unnecessary features from a dataset and retaining just the most important ones. The modified normative fish swarm (MNFS) approach is a metaheuristic optimization strategy that draws inspiration from the behavior of fish swarms. MNFS is specifically tailored for feature selection tasks, where it aims to identify the subset of features that maximizes the performance of DL model. The current state (AF) of the h-th P_h artificial fish and the food density in that state are Q_h the total number of neighborhood partners that satisfy the condition.

$$c_{hg} < visual \tag{8}$$

where b_F value denotes the h-th AF and the j-th neighbors distance is given by c_{hg}. In the visible and simulated behavior, when $b_F > 0$,then it will have one neighbor.

$$P_h^{s+1} = P_h^s + \frac{P_{Min} - P_h^s}{|P_{Min} - P_h^s|} Rand \times step \tag{9}$$

In the s-th iteration of h-th individual the position vector is indicated by P_h^s. The center position of the swarm is identified by counting all the neighbor buddies, and it is indicated by P_D, which has a centre fitness value as Q_D. When food density $P_D > P_h$ when $\frac{Q_D}{b_F} < \delta Q_h$, then count enhance collected swarm is given by:

$$P_h^{s+1} = P_h^s + \frac{P_D - P_h^s}{|P_D - P_h^s|} Rand \times step \tag{10}$$

AF performs random hunting behavior without checking any information from participants. A random position P_g is chosen in its realization scene.

$$P_g = P_h^s + Rand\,[-1,\ 1] \times visual \tag{11}$$

If $Q_g < Q_h$, this indicates high feed density P_g and the AF will advance to the designated spot.

$$P_h^{s+1} = P_h^s + \frac{P_g - P_h^s}{|P_g - P_h^s|} Rand \times step \tag{12}$$

It continues the hunting behavior until the maximum number of iterations is achieved in the failing situation where P_g offers a better food solution. The following is the expression for the updated speed vector characteristic of MNFS.

$$V_{s+1} = \omega V_s + rand\,[0,\ 1] \times step \left[\left(\frac{\xi_s \left(P_{jbest}^s - P_h^s \right) + \xi_{s-1} \left(P_{jbest}^{s-1} - P_h^{s-1} \right)}{\left| \xi_s \left(P_{jbest}^s - P_h^s \right) + \xi_{s-1} \left(P_{jbest}^{s-1} - P_h^{s-1} \right) \right|} \right) \right] \tag{13}$$

Indicates V_s the individual's speed in repetition, hence, V_{s+1} its updated velocity denotes the vector; (s - 1) represents P_h^s, the extreme value point representing the global optimum within the population during the initial iteration, and P_{jbest}^{s-1} indicates the current global extreme value of the P_{jbest}^s population throughout the iteration.

$$V_{s+1} = \omega V_s + rand\,[0,\ 1] \times step \left[\left(\frac{\xi_s \left(P_{lbest}^s - P_h^s \right) + \xi_{s-1} \left(P_{lbest}^{s-1} - P_h^{s-1} \right)}{\left| \xi_s \left(P_{lbest}^s - P_h^s \right) + \xi_{s-1} \left(P_{lbest}^{s-1} - P_h^{s-1} \right) \right|} \right) \right] \tag{14}$$

In this context, P_{lbest}^s; P_{lbest}^{s-1} signifies the intensity value associated with a single particle's position along the X-axis during the s-th iteration. The population of the function's global extreme value is represented by the (s - 1)-th.

$$B = H,\ U, L, C \tag{15}$$

Here, U, L, and C represent trajectories of dimensionality B, denoting upper, lower, and current positions respectively, for the locked break of variable K[(1, 2,..., B). This is depicted as follows..

$$H_K = [L_K,\ U_K] = \{P | L_K \le P \le U_K\} \tag{16}$$

The L_K and U_K represent the upper and lower limits of the executable domain for the K-th variable. Referring to Figure 2,L_K and U_K are initialized with the maximum and minimum bounds across the population and are subsequently adjusted according to the expressions outlined below.

$$L_K^{s+1} = \begin{cases} P_{h,K}, & P_{h,K} < L_K^s \ \ or \ \ F(P_h^s) < l_K^s \\ L_K^s, & otherwise \end{cases}$$

$$U_K^{s+1} = \begin{cases} P_{g,K}, & P_{g,K} < U_K^s \ \ or \ \ F(P_g^s) < U_K^s \\ U_K^s, & otherwise \end{cases} \tag{17}$$

Let P represent the population's state vector. The h-th individual influences the variable K's lower bound. The upper bound of the variable K is impacted by the g-th person.

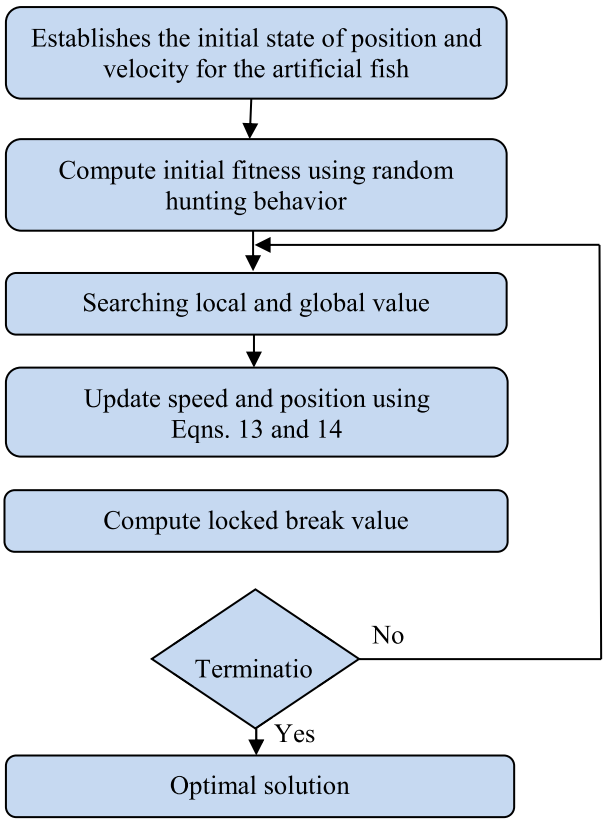

FIGURE 2. The Process of optimal feature selection using MNFS algorithm.

C. MULTIPLE NEUROLOGICAL BRAIN DISORDER DETECTION USING HHNN

The hinging hyperplane neural network (HHNN) is a specialized neural network architecture designed for the detection and classification of multiple neurological brain disorders, including neuro-typical conditions, epilepsy, and ASD. HHNN leverages a unique structure that enables it to effectively learn and discriminate between different patterns in complex data, such as EEG signals in the context of neurological disorders. Figure 3 shows the layer structure of HHNN, unlike traditional architectures that rely on linear or nonlinear activation functions, HHNN introduce a piecewise-linear activation function that allows more adaptive decision-making. We define the linear combination of maximum rule functions as follows.

$$F_{HH}(p) = \sum_{a=1}^{A} m_a N_a(p) \tag{18}$$

in which p $\in$ r^b is the input and F_{HH} $\in$ r is the output. In HHNN model, the basis function $N_a(p)$ takes the form of objective function as follows.

$$Max(0,\ L_a(p)\} \tag{19}$$

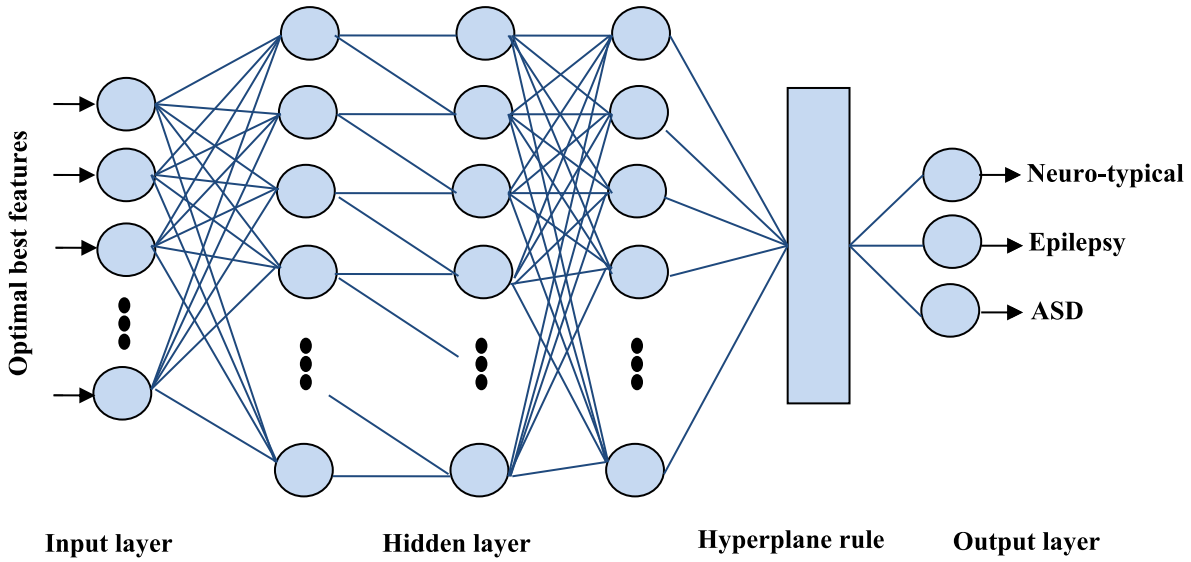

FIGURE 3. Proposed HHNN for multiple neurological brain disorder detection which consider the input as the optimal best features retrieved from pervious section.

in which $L_a(p)$ is a linear function. We utilize the commonly used ReLU activation function for rule formation in the linear function $L_a(p)$ to be p.

$$Max(0,\ L_a(p), \ldots, L_{K_b}(p)\} \tag{20}$$

with $K_b \leq$ b and $L_a(p)$, K= 1,…,K_b are linear. HHNN is linear combination of maximum rule functions and the basis function takes the form of fitness function.

$$N_a(p) = Min\{j_1(p), \ldots, j_k(p)\} \tag{21}$$

We define the control vector as follows.

$$j_K(p) - MAX\{0,\ t_K(p_{V_K} - \beta_K)\}, \quad K = 1, \ldots,\ k \tag{22}$$

where $t_K = \pm 1, V_1, \ldots..V_A$ are indices of the input variables, and $\beta_K \in [0, 1)$ are predefined scalars. Let $p = [p_1, \ldots..p_b]^S$ be the input variables. Other than the source nodes, the intermediate nodes can only accept inputs from the source in the hidden layer. Therefore, the output of a source node is expressed as follows.

$$bb_C(p) = MAX\{0,\ p_V - \beta_V\} \tag{23}$$

when V represents the input variable's index, and the offset is denoted by β_V. As a result, the weighted sum of the outputs from each neuron in the hidden layer is the HHNN's output.

$$F_{eii}(p) = \sum_{K=1}^{A} \alpha_K bb_{M_K}(p) + \alpha_0 \tag{24}$$

in which M_k is the neuron in the hidden layer, $bb_{M_K}(p)$ and $\alpha_K \in$ r denote the output and coefficient of the neuron M_k, K∈ {1,…, A}, and α_0 is the constant bias. The coefficients $\alpha_0, \alpha_1,\ldots,\alpha_A$ are called weights of the HHNN. We assume a node M_g receives inputs from the neurons M_{g_1}, M_{g_2}, i.e.,$bb_{M_g} = Min\{bb_{M_{g1}},\ bb_{M_{g2}}\}$. The same rule applies to $bb_{M_{g1}}$ and $bb_{M_{g2}}$, thus finally we can rewrite bb_{M_g} as follows.

$$bb_{M_g} = \underset{K \in k_g}{Min}\{bb_{M_K}\} \tag{25}$$

where k_g is the index set of source nodes connected either directly or indirectly. The basic function is stated as follows when compared to the HHNN.

$$N_M(p) = \underset{K \in k_a}{Min}\{MAX\{0,\ t_{Ka}(p_{VKa} - \beta_{Ka})\}\} \tag{26}$$

Let f: [0, 1] b → R be a continuous function. Then for any $\varepsilon >$ 0, there exists HHNN with a certain number of neurons, such that for all p ∈ [0, 1] b, we have the limit the rule as follows.

$$||F(p) - F_{eii}(p)|| < \varepsilon \tag{27}$$

A matrix of adjacency Each neuron's connections are represented by Ad, while the interactions between various input variables are described by the interaction matrix Ir.

$$HR = \begin{bmatrix} & C_1 & C_2 & C_3 & C_4 & D_1 & D_2 & D_3 & D_4 \\ C_1 & 0 & 0 & 0 & 0 & 1 & 1 & 1 & 1 \\ C_2 & 0 & 0 & 0 & 0 & 0 & 0 & 1 & 1 \\ C_3 & 0 & 0 & 0 & 0 & 1 & 0 & 1 & 0 \\ C_4 & 0 & 0 & 0 & 0 & 0 & 0 & 0 & 1 \\ D_1 & 0 & 0 & 0 & 0 & 0 & 0 & 0 & 0 \\ D_2 & 0 & 0 & 0 & 0 & 0 & 0 & 0 & 0 \\ D_3 & 0 & 0 & 0 & 0 & 0 & 0 & 0 & 0 \\ D_4 & 0 & 0 & 0 & 0 & 0 & 0 & 0 & 0 \end{bmatrix} \tag{28}$$

An interaction matrix *HR* is optimizes as follows.

$$F_{ehh}(p) = \alpha_0 + \sum_{h} \sum_{|T_{M_g}|=1} \alpha_g bb_{M_g}(p_h) + \sum_{h,K} \sum_{|T_{M_g}|=2} \alpha_g bb_{M_g}(p_h,\ p_K) + \ldots \tag{29}$$

where $|T_{M_g}|$ is the number of nonzero entries in Ir(:, g), or the number of elements in the set T_{M_g}. For instance, the following is the expression for each function in the first sum.

$$F_h(p_h) = \sum_{T_{M_g}=\{h\}} \alpha_g bb_{M_g}(p) \tag{30}$$

It is a sum over all source nodes involving the particular variable p_h. Each bivariate function in this second sum is expressed as follow.

$$F_{h,K}(p_h, p_K) = \sum_{T_{M_g}=\{h,K\}} \alpha_g bb_{M_g}(p) \tag{31}$$

This is the total of all the neurons involved in the specific pair of variables p_h and p_K. In a similar vein, all of the neurons involved in a given variable triple can be collected to determine the function of each rule in the third sum.

$$F_{h,K,R}(p_h, p_K, p_R) = \sum_{T_{M_g}=\{h,K,R\}} \alpha_g bb_{M_g}(p) \tag{32}$$

This gives the combined contribution of these three variables to the model when added to the respective univariate and bivariate functions, p_h, p_K, and p_R. To get the index j such that $T_{M_g} = \{h, K, R\}$, presuppose that the source nodes p_h, p_K and p_R include the variables $C_{\gamma h}$, $C_{\gamma K}$ *and* $C_{\gamma R}$. It is noted that such γ_h, γ_K *and* γ_R may not be unique.

$$HR_{\gamma h,g} = 1,\ HR_{\gamma h,g} = 1,\ HR_{\gamma h,g} = 1 \tag{33}$$

We have $T_{M_g} = \{h, K, R\}$. Interpretation of HHNN is greatly facilitated output layer. We observed that importance of the input variables of interactions among different input variables.

IV. RESULTS AND DISCUSSIONS

This section offers an examination of the results obtained by comparing the recommended RT-NeuroDDSM to other models that are currently in use for the diagnosis of neurological brain disorders. We employed publicly available datasets from King Abdulaziz University (KAU), CHB-MIT, and Bonn University in order to validate our proposed model. For implementation, Python version 3.6.9 was utilized, while the experiments were conducted using Google Colab Pro. The RT-NeuroDDSM was compared to a number of well-known models, including artificial neural networks (ANN), support vector machines (SVM), k-nearest neighbor (k-NN), and linear discriminant analysis (LDA).

A. DETAILS ON DATASET

To develop and evaluate our approaches, we used three different datasets, each with a special purpose in the diagnosis of epilepsy and autism. The first two datasets were centered on epilepsy diagnoses. The first dataset, which included the five sets named A, B, C, D, and E, was published for open access by Bonn University in Germany. There were precisely one hundred single-channel EEG signals in each batch. Sets C, D, and E were obtained from the intracranial EEGs of patients with epilepsy, whereas sets A and B were obtained from the scalp EEGs of Neurotypical people. Every signal was captured for about 23.6 seconds, with a sample frequency of 173.61 Hz. The second dataset comprised 906 hours of EEG data from 23 patients with epilepsy and was provided by the study team at MIT in the United States. This study contained data from the initial twelve autistic people as well as eleven neuro-typical subjects. This sample contained twenty-three EEG channels that were all recorded at 256 Hz. The third dataset came from the KAU Brain-Computer Interface (BCI) Research Group in Saudi Arabia, and focused on autism diagnosis. Each EEG signal was sent through two filters: a band-pass filter with a pass band of 0.1–60 Hz and a notch filter with a frequency stop band of 60 Hz. The duration of EEG data collection varied between 12 and 40 minutes for persons with autism and 5 to 27 minutes for patients displaying Neurotypical behavior. Digital conversion of the EEG signals resulted in a 256 Hz sample frequency. To address the duration discrepancy between the Bonn dataset (23.6 seconds) and the CHB-MIT dataset (longer recordings), we applied appropriate augmentation techniques for ECG signals to extend the Bonn dataset segments to 300 seconds. Specifically, we used noise addition methods, including Gaussian noise, salt-and-pepper noise, Poisson noise, and speckle noise, to create extended variations of the 23.6-second segments from the Bonn dataset. This approach allowed us to standardize all ECG recordings to a uniform duration of 300 seconds. For the CHB-MIT dataset, we segmented the longer recordings into 300-second intervals and annotated them accordingly. This ensured consistency and facilitated accurate comparisons across the datasets. Table 2 displays the summary of the dataset. One example of an EEG signal from the dataset is shown in Figure 4. Typically, 80% of the data is allocated for training, with the remaining 20% for testing.

The Bonn dataset is divided into five sets: Z (healthy subjects with eyes open), O (healthy subjects with eyes closed), N (interictal segments from patients), F (seizure-free intervals from epileptic patients), and S (ictal segments from epileptic patients). For our analysis, sets Z and O were considered normal, representing non-epileptic conditions. In contrast, sets N, F, and S were classified as epileptic, encompassing both interictal and ictal segments. This categorization allowed us to clearly distinguish between normal and epileptic EEG segments in our merged dataset, ensuring accurate and consistent annotations for our epilepsy classification model. To harmonize the Bonn and CHB-MIT datasets for our epilepsy classification study, we addressed differences in segment length and number of channels as follows: For segment length adjustment, each 23.6-second segment from the Bonn dataset was expanded to 300 seconds using data augmentation techniques, such as adding different types of noise. For the CHB-MIT dataset, each recording was segmented into multiple 300-second segments. Regarding channel harmonization, the single-channel data from the Bonn dataset was used as is, while from the multi-channel CHB-MIT recordings, a single representative channel was selected, typically the

TABLE 2. Summary of dataset.

Description	Dataset		
	CHB-MIT	Bonn University	KAU-BCI
Subjects	22	10	15
Attacks/Events	87	500	NA
Signal recording types	Scalp EEG	Intracranial EEG	Scalp EEG
Sampling frequency (Hz)	256	256	256
Total time consider (seconds)	300	300	300
Classes	Healthy/Epilepsy	Healthy/Epilepsy	Healthy/Autism

TABLE 3. Accuracy comparison of various models for feature extraction in neurological brain disorders diagnosis.

Feature extraction+detection model	Binary classification			Two class classification			Multi class classification
	Healthy	Epilepsy	Autism	Healthy and Epilepsy	Healthy and Autism	Epilepsy and Autism	All 3 disease
DWT+LBP+LDA	95.235	93.672	92.109	99.522	84.052	68.582	99.025
DWT+LBP+SVM	94.785	93.222	91.659	99.532	85.232	70.932	99.752
DWT+LBP+KNN	95.102	93.539	91.976	99.514	90.412	81.310	99.142
DWT+LBP+ANN	94.478	92.915	91.352	99.536	91.245	82.954	77.235
DWT+SD+LDA	95.378	93.815	92.252	90.012	74.415	58.818	96.945
DWT+SD+SVM	95.636	94.073	92.510	99.125	82.752	66.379	98.341
DWT+SD+KNN	94.852	93.289	91.726	99.235	88.024	76.813	96.214
DWT+SD+ANN	94.312	92.749	91.186	95.247	89.425	83.603	60.754
DWT+Varaiance+LDA	94.365	92.802	91.239	80.025	49.125	18.225	65.526
DWT+Varaiance+SVM	85.475	83.912	82.349	92.125	75.504	58.883	96.978
DWT+Varaiance+KNN	86.314	84.751	83.188	99.178	85.302	71.426	73.314
DWT+Varaiance+ANN	88.635	87.072	85.509	66.524	63.874	61.224	58.302
DWT+Kurtosis+LDA	87.863	86.300	84.737	90.278	58.412	26.546	67.584
DWT+Kurtosis+SVM	87.091	85.528	83.965	96.147	79.212	62.277	84.725
DWT+Kurtosis+KNN	86.319	84.756	83.193	95.347	78.356	61.365	84.463
DWT+Kurtosis+ANN	85.547	83.984	82.421	95.635	86.201	76.767	97.968
DWT+Entropy+LDA	89.647	88.084	86.521	99.524	86.224	72.924	99.923
DWT+Entropy+SVM	84.158	82.595	81.032	99.536	90.518	81.500	98.475
DWT+Entropy+KNN	88.235	86.672	85.109	95.541	90.834	86.127	98.725
DWT+Entropy+ANN	87.452	85.889	84.326	99.523	78.568	57.613	94.528
TCSNet+MNFS+HHNN	99.523	99.610	99.357	99.745	99.245	99.369	99.812

Fz-Cz channel. For annotation, sets Z and O from the Bonn dataset were considered normal, while sets N, F, and S were considered epileptic. For the CHB-MIT dataset, annotations were preserved based on the original seizure labels for each 300-second segment. This harmonization process ensured consistency across datasets, enabling effective epilepsy classification.

B. RESULTS COMPARISON OF FEATURE EXTRACTION TECHNIQUES

Table 3 shows the accuracy comparison of different models designed for feature extraction in diagnosing neurological brain disorders. For the "Healthy" category, which involves individuals without neurological disorders, the model achieved high accuracy scores ranging from 99.357% to 99.610% across different evaluations. In the case of "Epilepsy" diagnosis, where patients exhibit abnormal brain activity characteristic of epilepsy, the "TCSNet+MNFS+HHNN" model attained accuracy scores ranging from 99.245% to 99.745%. Moreover, the model's performance in identifying combined categories, such as "Healthy and Epilepsy," "Healthy and Autism," "Epilepsy and Autism," and "All 3 diseases," was also evaluated. Across these combined categories,

TABLE 4. Comparative analysis of various methods for neurological brain disorders diagnosis for binary class classification.

Method	Values in %				
	Accuracy	Precision	Recall	F-measure	AUC
	Healthy				
LDA	98.243	95.514	95.383	95.448	95.794
SVM	98.678	95.949	95.818	95.884	96.229
KNN	99.114	96.385	96.254	96.319	96.665
ANN	99.549	96.820	96.689	96.755	97.100
HHNN	99.985	97.256	97.125	97.190	97.536
	Epilepsy disease				
LDA	96.710	93.981	93.850	93.915	94.261
SVM	97.146	94.417	94.286	94.351	94.697
KNN	97.581	94.852	94.721	94.787	95.132
ANN	98.017	95.288	95.157	95.222	95.568
HHNN	98.452	95.723	95.592	95.658	96.003
	Autism disease				
LDA	93.814	91.085	90.954	91.019	91.365
SVM	94.250	91.521	91.390	91.455	91.801
KNN	94.685	91.956	91.825	91.891	92.236
ANN	95.121	92.392	92.261	92.326	92.672
HHNN	95.556	92.827	92.696	92.762	93.107

the ''TCSNet+MNFS+HHNN'' model consistently yielded high accuracy scores ranging from 99.245% to 99.812%, underscoring its robustness in diagnosing multiple neurological conditions simultaneously. Compared to other techniques [33], [34], [35], the results underscore the efficacy of the ''TCSNet+MNFS+HHNN'' model in accurately extracting features from EEG signals and diagnosing various neurological disorders with a high degree of accuracy, thereby offering promising prospects for advancing clinical diagnosis and treatment planning in neurology.

C. RESULTS COMPARISON OF VARIOUS METHODS FOR NEUROLOGICAL BRAIN DISORDERS DIAGNOSIS

Table 4 provides a comprehensive comparison of various methods utilized in the diagnosis of neurological brain disorders, focusing on binary class classification for three distinct conditions: Healthy, Epilepsy, and Autism. The analysis of the results reveals notable differences in the performance metrics across different methods for each disease category. Starting with the Healthy classification, the model exhibits the highest accuracy, achieving an impressive 99.985%. Figure 5 represents a substantial increase of approximately 1.436% compared to the next best-performing method, the ANN. Additionally, HHNN demonstrates notable improvements in precision, recall, F-measure, and AUC score, with increases ranging from approximately 0.736% to 1.742% compared to other methods. Moving on to Epilepsy disease classification, the HHNN model continues to show superior performance, achieving an accuracy of 98.452%. Figure 6 represents a substantial increase of approximately 0.465% compared to the next best-performing method, the ANN. For Autism disease classification, the HHNN model maintains its dominance with an accuracy of 95.556%, shows notable increase of approximately 0.635% compared to the ANN, the next best-performing method.

Figure 7 shows similar to the other disease categories, HHNN exhibits increases in precision, recall, F-measure, and AUC score compared to alternative methods, ranging from approximately 0.435% to 0.742%.Overall, the HHNN model consistently demonstrates superior performance across all disease categories, with increases ranging from approximately 0.364% to 1.742% compared to alternative methods in terms of accuracy, precision, recall, F-measure, and AUC score.

Table 5 presents a comparative analysis of various methods for the diagnosis of neurological brain disorders, focusing on two-class scenarios, Healthy and Epilepsy, Healthy and Autism, and Epilepsy and Autism. In the Healthy and Epilepsy classification, the HHNN model demonstrates exceptional accuracy, achieving an impressive 99.856%. Figure 8 shows a substantial increase of approximately 5.632% compared to the next best-performing method, the ANN. Moreover, HHNN exhibits substantial increases in precision, recall, F-measure, and AUC score, ranging from

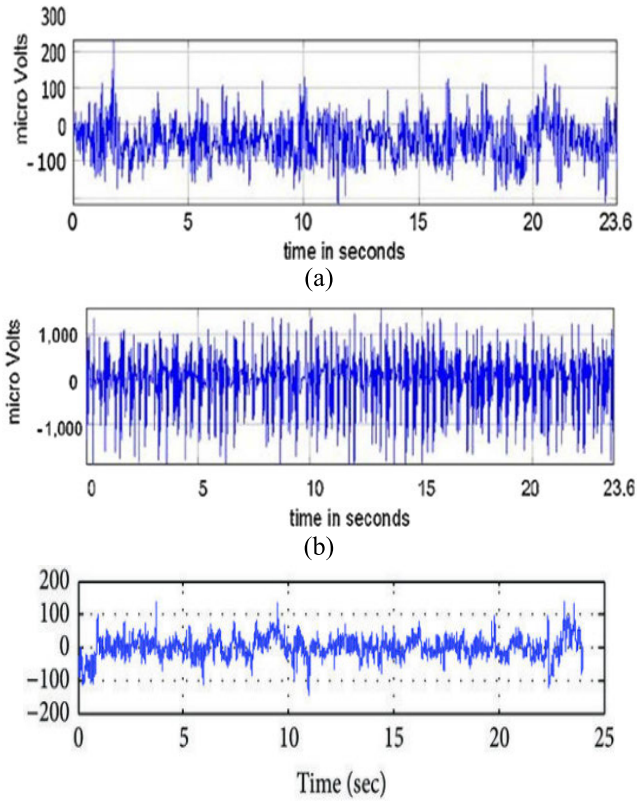

FIGURE 4. The Test sample from dataset with EEG signals of (a) Neuro-typical disease (b) Epilepsy disease (c) Autism disease.

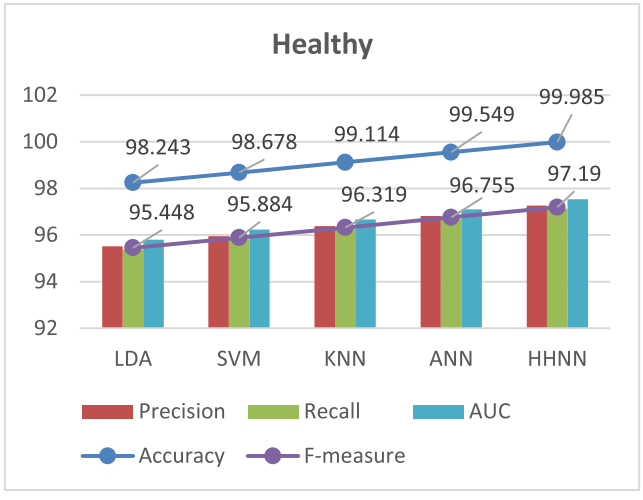

FIGURE 5. Results comparison for detection of healthy.

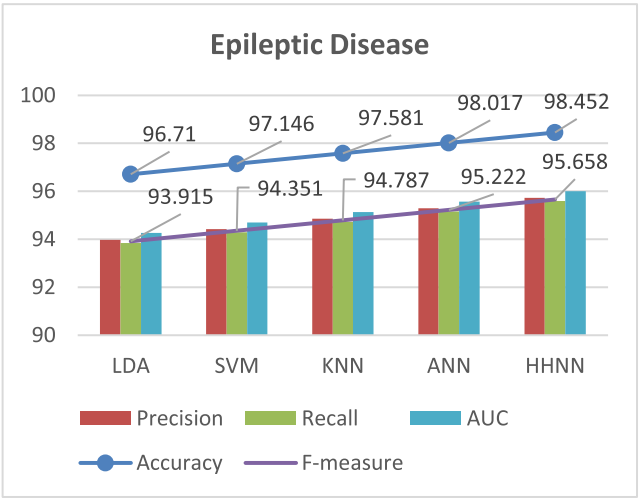

FIGURE 6. Results comparison for detection of epilepsy disease.

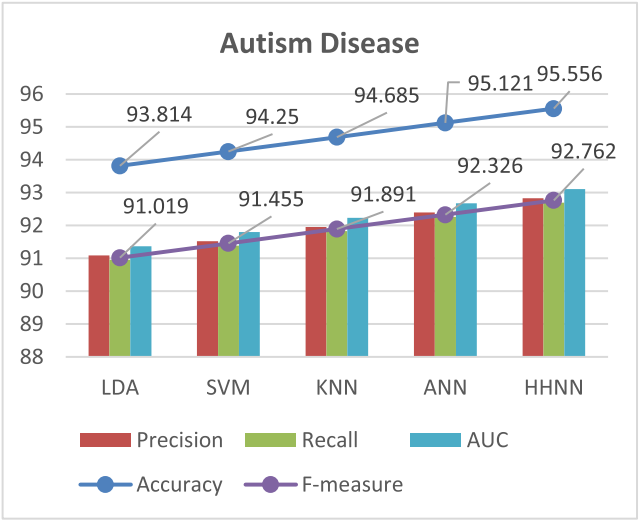

FIGURE 7. Results comparison for detection of autism disease.

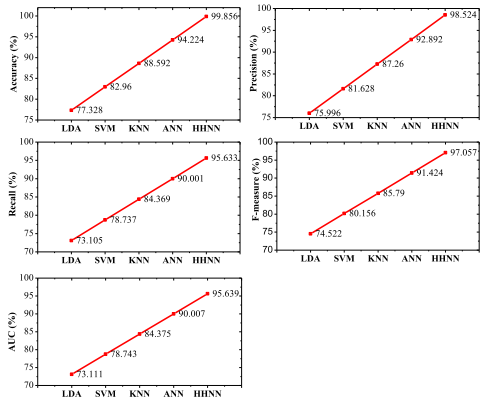

FIGURE 8. Results comparison for detection of healthy and epilepsy disease.

approximately 3.531% to 5.926% compared to alternative methods. For the Healthy and Autism classification, the HHNN model again exhibits superior performance, achieving an accuracy of 99.398%. Figure 9 shows an increase of approximately 5.632% compared to the ANN, the next best-performing method. Additionally, HHNN shows significant increases in precision, recall, F-measure, and AUC score compared to alternative methods, ranging from approximately 3.517% to 5.848%.

TABLE 5. Comparative analysis of various methods for neurological brain disorders diagnosis for two class classification.

Method	Values in %				
	Accuracy	Precision	Recall	F-measure	AUC
	Healthy and Epilepsy				
LDA	77.328	75.996	73.105	74.522	73.111
SVM	82.960	81.628	78.737	80.156	78.743
KNN	88.592	87.260	84.369	85.790	84.375
ANN	94.224	92.892	90.001	91.424	90.007
HHNN	99.856	98.524	95.633	97.057	95.639
	Healthy and Autism				
LDA	76.870	75.538	72.647	74.064	72.653
SVM	82.502	81.170	78.279	79.698	78.285
KNN	88.134	86.802	83.911	85.332	83.917
ANN	93.766	92.434	89.543	90.966	89.549
HHNN	99.398	98.066	95.175	96.599	95.181
	Epilepsy and Autism				
LDA	77.099	75.767	72.876	74.293	72.882
SVM	82.731	81.399	78.508	79.927	78.514
KNN	88.363	87.031	84.140	85.561	84.146
ANN	93.995	92.663	89.772	91.195	89.778
HHNN	99.627	98.295	95.404	96.828	95.410

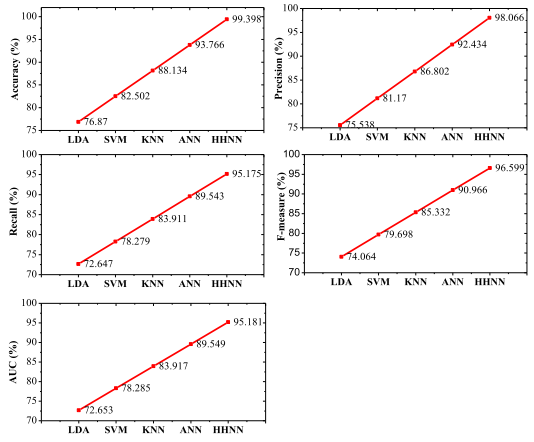

FIGURE 9. Results comparison for detection of healthy and autism disease.

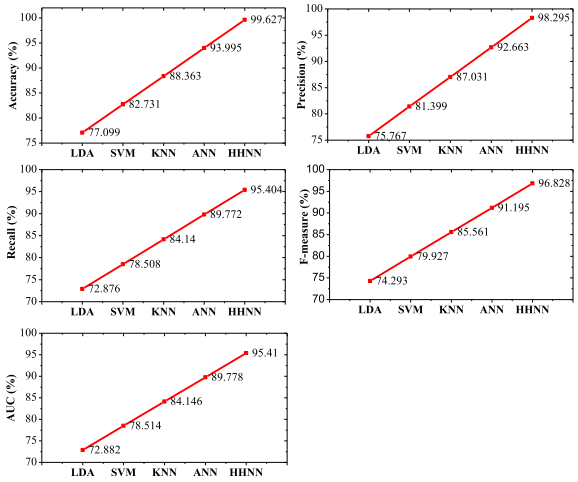

FIGURE 10. Results comparison for detection of epilepsy and autism disease.

In the Epilepsy and Autism classification, the HHNN model maintains its dominance with an accuracy of 99.627%, shows a substantial increase of 5.632% compared to the ANN, the next best-performing method. Figure 10 shows, HHNN exhibits notable increases in precision, recall, F-measure, and AUC score compared to other methods, ranging from approximately 3.522% to 5.836%.HHNN model outperforms alternative methods across all classification tasks, with increases ranging from approximately 3.517% to 5.926% compared to other methods in terms of accuracy, precision, recall, F-measure, and AUC score. The results underscore the effectiveness of the HHNN approach in accurately diagnosing various neurological brain disorders in two-class classification scenarios.

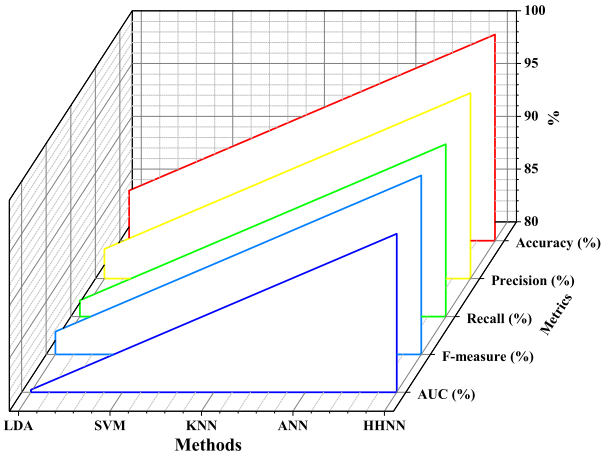

FIGURE 11. Results comparison for detection of multi-disease (healthy, epilepsy and autism).

Table 6 provides a comparative analysis of various methods for the diagnosis of neurological brain disorders using multi-class classification. The same is visualized in Figure 11. In terms of accuracy, HHNN model outperforms other methods with a remarkable accuracy of 99.548%. It represents a substantial increase of approximately 3.698% compared to the next best-performing method, the ANN. HHNN also demonstrates significant increases in precision, recall, F-measure, and AUC score compared to alternative methods, ranging from approximately 3.698% to 4.225%. SVM follows closely behind HHNN in terms of accuracy, achieving an accuracy of 88.454%.

TABLE 6. Comparative analysis of various methods for neurological brain disorders diagnosis for multi class classification.

Method	Values in %				
	Accuracy	Precision	Recall	F-score	AUC
LDA	84.756	82.797	81.533	82.160	80.236
SVM	88.454	86.495	85.231	85.858	83.934
KNN	92.152	90.193	88.929	89.557	87.632
ANN	95.850	93.891	92.627	93.255	91.330
HHNN	99.548	97.589	96.325	96.953	95.028

While SVM exhibits lower accuracy compared to HHNN, it still shows competitive performance across other metrics, with increases ranging from approximately 2.701% to 3.924% compared to alternative methods. KNN and ANN also show respectable performance in terms of accuracy, achieving 92.152% and 95.850% respectively. However, both methods exhibit lower accuracy compared to HHNN and SVM. KNN and ANN demonstrate increases ranging from approximately 3.300% to 4.044% and 0.696% to 1.921% respectively compared to alternative methods across other metrics. Lastly, LDA exhibits the lowest accuracy among the methods evaluated, achieving an accuracy of 84.756%. Despite its lower accuracy, LDA still shows competitive performance in terms of precision, recall, F-measure, and AUC score, with increases ranging from approximately 1.269% to 3.523% compared to alternative methods.

V. CONCLUSION

We have developed an innovative IoMT-based real-time diagnosis model, RT-NeuroDDSM, for the detection of neurological brain disorders. It integrates systematic deep learning techniques with EEG signals to enable accurate and efficient diagnosis. The TCSNet architecture is employed for feature extraction, allowing the extraction of high-level time series, channel, and spatial features from EEG data. MNFS algorithm is used for feature selection, optimizing the feature set to enhance classification performance. HHNN model serves as the primary classifier, effectively detect multiple neurological disorders including healthy, epilepsy, and ASD. To validate the effectiveness of our model, we conducted experiments using publicly available EEG datasets such as those from University of Bonn-Germany, CHB-MIT repository, and KAU-Saudi Arabia. The results show outstanding performance, with RT-NeuroDDSM achieving an overall classification accuracy of 99.607%. This represents a significant improvement of 5.471% over existing state-of-the-art models. Moreover, RT-NeuroDDSM achieves impressive precision, recall, and F-measure values of 98.119%, 95.634%, and 96.895% respectively. While the RT-NeuroDDSM model shows significant promise in real-time diagnosis of neurological disorders, there are several areas for improvement and future research. One limitation is the reliance on publicly available EEG datasets, which may not fully represent global patient diversity. Expanding the dataset to include more diverse samples could enhance generalizability. Additionally, integrating multimodal data sources, such as MRI or CT scans, could further improve diagnostic accuracy. Future work should also focus on optimizing the model for scalability and real-world deployment, ensuring it can handle large volumes of data and integrate into existing healthcare systems. Personalizing the model to adapt to individual patient characteristics and addressing potential biases are crucial for improving diagnostic precision. Longitudinal studies to assess long-term performance and impact on patient outcomes would provide valuable insights, while ensuring compliance with regulatory and ethical standards will be essential for clinical adoption.

DECLARATION OF INTEREST

The authors declare that they have no conflict of interest.

REFERENCES

[1] D. M. Mathkor, N. Mathkor, Z. Bassfar, F. Bantun, P. Slama, F. Ahmad, and S. Haque, "Multirole of the Internet of Medical Things (IoMT) in biomedical systems for managing smart healthcare systems: An overview of current and future innovative trends," *J. Infection Public Health*, vol. 17, no. 4, pp. 559–572, Apr. 2024, doi: 10.1016/j.jiph.2024.01.013.

[2] S. F. Ahmed, M. S. B. Alam, S. Afrin, S. J. Rafa, N. Rafa, and A. H. Gandomi, "Insights into Internet of Medical Things (IoMT): Data fusion, security issues and potential solutions," *Inf. Fusion*, vol. 102, Feb. 2024, Art. no. 102060, doi: 10.1016/j.inffus.2023.102060.

[3] K. K. Baseer, K. Sivakumar, D. Veeraiah, G. Chhabra, P. K. Lakineni, M. J. Pasha, R. Gandikota, and G. Harikrishnan, "Healthcare diagnostics with an adaptive deep learning model integrated with the Internet of Medical Things (IoMT) for predicting heart disease," *Biomed. Signal Process. Control*, vol. 92, Jun. 2024, Art. no. 105988, doi: 10.1016/j.bspc.2024.105988.

[4] M. A. Jan, W. Zhang, F. Khan, S. Abbas, and R. Khan, "Lightweight and smart data fusion approaches for wearable devices of the Internet of Medical Things," *Inf. Fusion*, vol. 103, Mar. 2024, Art. no. 102076, doi: 10.1016/j.inffus.2023.102076.

[5] J. Liu, W. Cui, Y. Chen, Y. Ma, Q. Dong, R. Cai, Y. Li, and B. Hu, "Deep fusion of multi-template using spatio-temporal weighted multi-hypergraph convolutional networks for brain disease analysis," *IEEE Trans. Med. Imag.*, vol. 43, no. 2, pp. 860–873, Feb. 2024, doi: 10.1109/TMI.2023.3325261.

[6] L. Qian, J. Lu, W. Li, Y. Huan, Y. Sun, L. Zheng, and Z. Zou, "MCU-enabled epileptic seizure detection system with compressed learning," *IEEE Internet Things J.*, vol. 11, no. 5, pp. 8771–8782, Mar. 2024, doi: 10.1109/JIOT.2023.3323264.

[7] C. Wang, L. Liu, W. Zhuo, and Y. Xie, "An epileptic EEG detection method based on data augmentation and lightweight neural network," *IEEE J. Transl. Eng. Health Med.*, vol. 12, pp. 22–31, 2024, doi: 10.1109/JTEHM.2023.3308196.

[8] Y. Yang, C. Ye, X. Guo, T. Wu, Y. Xiang, and T. Ma, "Mapping multimodal brain connectome for brain disorder diagnosis via cross-modal mutual learning," *IEEE Trans. Med. Imag.*, vol. 43, no. 1, pp. 108–121, Jan. 2024, doi: 10.1109/TMI.2023.3294967.

[9] N. S. Amer and S. B. Belhaouari, "EEG signal processing for medical diagnosis, healthcare, and monitoring: A comprehensive review," *IEEE Access*, vol. 11, pp. 143116–143142, 2023, doi: 10.1109/ACCESS.2023.3341419.

[10] S. Kumar, N. K. Garg, A. Jain, P. Pandey, A. Khopade, and K. K. Sawant, "Emerging therapeutic landscape on delivery of oxytocin to brain for treating neurological disorders," *J. Drug Del. Sci. Technol.*, vol. 92, Feb. 2024, Art. no. 105370, doi: 10.1016/j.jddst.2024.105370.

[11] J. Sanchis, S. García-Ponsoda, M. A. Teruel, J. Trujillo, and I.-Y. Song, "A novel approach to identify the brain regions that best classify ADHD by means of EEG and deep learning," *Heliyon*, vol. 10, no. 4, Feb. 2024, Art. no. e26028, doi: 10.1016/j.heliyon.2024.e26028.

[12] T. Islam, M. Basak, R. Islam, and A. D. Roy, "Investigating population-specific epilepsy detection from noisy EEG signals using deep-learning models," *Heliyon*, vol. 9, no. 12, Dec. 2023, Art. no. e22208, doi: 10.1016/j.heliyon.2023.e22208.

[13] J. R. Martin and S. L. Swapna, "A machine learning framework for epileptic seizure detection by analyzing EEG signals," *Int. J. Comput. Digit. Syst.*, vol. 11, no. 1, pp. 1383–1391, Apr. 2022, doi: 10.12785/ijcds/1101112.

[14] O. S. Lih, V. Jahmunah, E. E. Palmer, P. D. Barua, S. Dogan, T. Tuncer, S. García, F. Molinari, and U. R. Acharya, "EpilepsyNet: Novel automated detection of epilepsy using transformer model with EEG signals from 121 patient population," *Comput. Biol. Med.*, vol. 164, Sep. 2023, Art. no. 107312, doi: 10.1016/j.compbiomed.2023.107312.

[15] M. Shen, P. Wen, B. Song, and Y. Li, "Real-time epilepsy seizure detection based on EEG using tunable-Q wavelet transform and convolutional neural network," *Biomed. Signal Process. Control*, vol. 82, Apr. 2023, Art. no. 104566, doi: 10.1016/j.bspc.2022.104566.

[16] S. Qiu, W. Wang, and H. Jiao, "LightSeizureNet: A lightweight deep learning model for real-time epileptic seizure detection," *IEEE J. Biomed. Health Informat.*, vol. 27, no. 4, pp. 1845–1856, Apr. 2023, doi: 10.1109/JBHI.2022.3223970.

[17] S. N. S. Fakhari, F. Ghaderi, M. Tehrani-Doost, and N. M. Charkari, "EEG-based brain connectivity analysis in autism spectrum disorder: Unraveling the effects of bumetanide treatment," *Biomed. Signal Process. Control*, vol. 86, Sep. 2023, Art. no. 105054, doi: 10.1016/j.bspc.2023.105054.

[18] M. Romero-González, P. Navas-Sánchez, E. Marín-Gámez, M. A. Barbancho-Fernández, V. E. Fernández-Sánchez, J. P. Lara-Muñoz, and J. Guzmán-Parra, "EEG abnormalities and clinical phenotypes in pre-school children with autism spectrum disorder," *Epilepsy Behav.*, vol. 129, Apr. 2022, Art. no. 108619, doi: 10.1016/j.yebeh.2022.108619.

[19] C. Piazza, C. Dondena, E. M. Riboldi, V. Riva, and C. Cantiani, "Baseline EEG in the first year of life: Preliminary insights into the development of autism spectrum disorder and language impairments," *iScience*, vol. 26, no. 7, Jul. 2023, Art. no. 106987, doi: 10.1016/j.isci.2023.106987.

[20] J. K. Singh and D. Kakkar, "Chronological sewing training optimization enabled deep learning for autism spectrum disorder using EEG signal," *Multimedia Tools Appl.*, Feb. 2024, doi: 10.1007/s11042-024-18341-6.

[21] K. M. Alalayah, E. M. Senan, H. F. Atlam, I. A. Ahmed, and H. S. A. Shatnawi, "Effective early detection of epileptic seizures through EEG signals using classification algorithms based on t-distributed stochastic neighbor embedding and K-means," *Diagnostics*, vol. 13, no. 11, p. 1957, Jun. 2023, doi: 10.3390/diagnostics13111957.

[22] M. K. Alharthi, K. M. Moria, D. M. Alghazzawi, and H. O. Tayeb, "Epileptic disorder detection of seizures using EEG signals," *Sensors*, vol. 22, no. 17, p. 6592, Aug. 2022, doi: 10.3390/s22176592.

[23] S. U. Khan, S. U. Jan, and I. Koo, "Robust epileptic seizure detection using long short-term memory and feature fusion of compressed time–frequency EEG images," *Sensors*, vol. 23, no. 23, p. 9572, Dec. 2023, doi: 10.3390/s23239572.

[24] Z. Lasefr, K. Elleithy, R. R. Reddy, E. Abdelfattah, and M. Faezipour, "An epileptic seizure detection technique using EEG signals with mobile application development," *Appl. Sci.*, vol. 13, no. 17, p. 9571, Aug. 2023, doi: 10.3390/app13179571.

[25] S. Mekruksavanich and A. Jitpattanakul, "Effective detection of epileptic seizures through EEG signals using deep learning approaches," *Mach. Learn. Knowl. Extraction*, vol. 5, no. 4, pp. 1937–1952, Dec. 2023, doi: 10.3390/make5040094.

[26] Y. Sun and X. Chen, "Epileptic EEG signal detection using variational modal decomposition and improved grey wolf algorithm," *Sensors*, vol. 23, no. 19, p. 8078, Sep. 2023, doi: 10.3390/s23198078.

[27] J. H. Lee, G. W. Lee, G. Bong, H. J. Yoo, and H. K. Kim, "Deep-learning-based detection of infants with autism spectrum disorder using auto-encoder feature representation," *Sensors*, vol. 20, no. 23, p. 6762, Nov. 2020, doi: 10.3390/s20236762.

[28] T.-H. Pham, J. Vicnesh, J. K. E. Wei, S. L. Oh, N. Arunkumar, E. W. Abdulhay, E. J. Ciaccio, and U. R. Acharya, "Autism spectrum disorder diagnostic system using HOS bispectrum with EEG signals," *Int. J. Environ. Res. Public Health*, vol. 17, no. 3, p. 971, Feb. 2020, doi: 10.3390/ijerph17030971.

[29] J. J. Esqueda-Elizondo, R. Juárez-Ramírez, O. R. López-Bonilla, E. E. García-Guerrero, G. M. Galindo-Aldana, L. Jiménez-Beristáin, A. Serrano-Trujillo, E. Tlelo-Cuautle, and E. Inzunza-González, "Attention measurement of an autism spectrum disorder user using EEG signals: A case study," *Math. Comput. Appl.*, vol. 27, no. 2, p. 21, Mar. 2022, doi: 10.3390/mca27020021.

[30] K. K. Mujeeb Rahman and M. M. Subashini, "Identification of autism in children using static facial features and deep neural networks," *Brain Sci.*, vol. 12, no. 1, p. 94, Jan. 2022, doi: 10.3390/brainsci12010094.

[31] S. Alhassan, A. Soudani, and M. Almusallam, "Energy-efficient EEG-based scheme for autism spectrum disorder detection using wearable sensors," *Sensors*, vol. 23, no. 4, p. 2228, Feb. 2023, doi: 10.3390/s23042228.

[32] S. Peketi and S. B. Dhok, "Machine learning enabled P300 classifier for autism spectrum disorder using adaptive signal decomposition," *Brain Sci.*, vol. 13, no. 2, p. 315, Feb. 2023, doi: 10.3390/brainsci13020315.

[33] F. A. Alturki, K. AlSharabi, A. M. Abdurraqeeb, and M. Aljalal, "EEG signal analysis for diagnosing neurological disorders using discrete wavelet transform and intelligent techniques," *Sensors*, vol. 20, no. 9, p. 2505, Apr. 2020, doi: 10.3390/s20092505.

[34] T. Bhattacharya, G. A. B. E. Soares, H. Chopra, M. M. Rahman, Z. Hasan, S. S. Swain, and S. Cavalu, "Applications of phyto-nanotechnology for the treatment of neurodegenerative disorders," *Materials*, vol. 15, no. 3, p. 804, Jan. 2022, doi: 10.3390/ma15030804.

[35] A. K. Rehni, N. Singh, and A. S. Jaggi, "Possible involvement of insulin, endogenous opioids and calcitonin gene related peptide in remote ischaemic preconditioning of brain," *Yakugaku Zasshi*, vol. 127, no. 6, pp. 1013–1020, Jun. 2007, doi: 10.1248/yakushi.127.1013.

RUCHI MITTAL is a professional with over two decades of work experience in teaching, training, research, and academic administration. Her teaching expertise comprises of DBMS, machine learning, social networking analysis, and data mining. She has published over 40 papers in Scopus/SCI indexed journals, book series, and conference proceedings. She received the Chitkara University Research Excellence Award in author with highest H-index category in 2020 (Computer Applications Discipline). She currently reviews a number of leading international journals, such as *Internet Research* (Emerald), *World Review of Science, Technology and Sustainable Development* (Inderscience), *International Journal of Computational Science and Engineering* (Inderscience), *International Journal of Intelligent Systems Technologies and Applications* (Inderscience), and a number of IEEE and Springer conferences. She serves on the TPC for a number of conferences and is an active Ph.D. advisor.

R. JOHN MARTIN received the Ph.D. degree in computer science from Bharathiar University, India, with a focus on an innovative machine learning model for epileptic seizure detection using EEG signals. He holds expertise in machine learning, healthcare AI, and signal processing, spanning a 27-year career in higher education, research, and educational leadership. He is currently with Jazan University, Saudi Arabia, he's known for his pedagogical talent and administrative leadership. He is a Distinguished Educator of computer science. His impactful works feature in prestigious journals of IEEE and ACM. Notably, he holds international patents and copyrights, showcasing ground-breaking healthcare AI innovations.

HAMDAN ALSHEHRI received the M.Sc. degree in computer and information science from Cleveland State University, Cleveland, OH, USA, in 2014, and the D.Sc. degree in information technology from Towson University, Towson, MD, USA, in 2014. He is currently an Assistant Professor with the College of Computer Science and Information Technology, Jazan University, Saudi Arabia. His research interests include data analysis, data visualization, and machine learning.

VARUN MALIK (Member, IEEE) received the Ph.D. degree in computer science and engineering from I.K. Gujral Punjab Technical University, Punjab, India. He is holding more than ten Indian patents/copyrights. His current research interests include blockchain, artificial intelligence, cloud computing, cyber security, the Internet of Things, data mining and warehousing, and method engineering. He is serving as a reviewer for many international journals.

S. B. GOYAL (Senior Member, IEEE) received the Ph.D. degree in computer science and engineering from Banasthali University, Rajasthan, India, in 2012. He is currently the Director of the Faculty of Information Technology, City University Malaysia. He served many institutions in many different academic and administrative positions. He is holding more than 20 years of work experience at national and international levels. He has peerless inquisitiveness and enthusiasm to get abreast with the latest development in the IT field. He has good command over industry revolution (IR) 4.0 technologies, such as big data, data science, artificial intelligence and blockchain, and cloud computing. He is the first one to introduce IR 4.0, including blockchain technology in the academic curriculum in Malaysian universities. He had participated in many panel discussions on IR 4.0 technologies at academia as well as industry platforms. He had contributed in many Scopus/SCI journals/conferences. He is holding more than ten international patents/copyrights from Australia, Germany, and India. His current research interests include blockchain, artificial intelligence, cloud computing, cyber security, the Internet of Things, data mining and warehousing, and method engineering.

S. L. SWAPNA received the master's and M.Phil. degrees in computer science from Manonmaniam Sundaranar University, India, and the Ph.D. degree in computer science from Bharathiar University, Coimbatore, India. She is currently an Academician and a Technical Trainer. She is also a Professional IT Trainer with Applexus Technologies, Thiruvananthapuram. Previously, she was a Faculty Member with the School of Engineering and Computer Science, Jazan University, Saudi Arabia. Her research interests include big data, machine learning, predictive data analytics, and privacy preserved data security.

HAITHAM ASSIRI received the bachelor's degree in information systems from King Khalid University, Abha, Saudi Arabia, in 2012, the master's degree in computer science technology from Kentucky State University, Frankfort, KY, USA, in 2016, and the Ph.D. degree in information systems from the University of Technology Sydney, New South Wales, Australia, in 2022. Additionally, he was an Assistant Faculty Member with the University of Technology Sydney, from 2019 to 2020. He is currently an Associate Professor with the College of Engineering and Computer Science, Jazan University, Saudi Arabia. His research interests include information and computer security, cybersecurity, cryptography, information security, and blockchain technology.

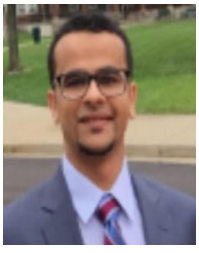

SALAHALDEEN DURAIBI (Member, IEEE) received the B.S. degree in computer science from Jazan University, Saudi Arabia, the M.S. degree in computer science from Kentucky State University, USA, and the Ph.D. degree in computer science from the University of Idaho, USA. He is currently an Assistant Professor with the College of Computer Science and Information Technology, Jazan University, Saudi Arabia. His research interests include computer and network security, intrusion detection, AI, and ML.